Journal of Materials Chemistry A

Boosted piezoelectricity with excellent thermal stability in tetragonal $NaNbO_3$-based ceramics

Journal:	*Journal of Materials Chemistry A*
Manuscript ID	TA-ART-10-2020-010470.R1
Article Type:	Paper
Date Submitted by the Author:	04-Dec-2020
Complete List of Authors:	Wang, Lu; University of Science and Technology Beijing, Department of Physical Chemistry Sun, Shengdong; University of Science and Technology Beijing Luo, Huajie; University of Science and Technology Beijing, Department of Physical Chemistry Ren, Yang; Argonne National Laboratory, X-ray Science Division Liu, Hui; University of Science and Technology Beijing, Xing, Xianran; University of Science and Technology Beijing, School of Metallurgical and Ecological Engineering Chen, Jun; University of Science and Technology Beijing, Department of Physical Chemistry

ARTICLE

Boosted piezoelectricity with excellent thermal stability in tetragonal $NaNbO_3$-based ceramics

Received 00th January 20xx,
Accepted 00th January 20xx

DOI: 10.1039/x0xx00000x

Lu Wang,[a] Shengdong Sun,[a] Huajie Luo,[a] Yang Ren,[c] Hui Liu,*[a] Xianran Xing [a] and Jun Chen*[a,b]

The realization of high piezoelectric performance and excellent temperature stability simultaneously in lead-free ceramics is the key for replacing Pb-containing perovskites in industry. In this study, large piezoelectric performance (d_{33} = 354 pC/N) was achieved in a wide temperature sinterable potassium-free $NaNbO_3$-$BaTiO_3$-$BaSnO_3$ system, which is twice more than the piezoelectricity found in $NaNbO_3$-$BaTiO_3$ binary ceramics. Structural refinement of high energy synchrotron powder diffraction suggests a single tetragonal structure with *P4bm* symmetry for the studied $NaNbO_3$-based lead-free ceramic. The results indicate that the small axial ratio favoring polarization reorientation benefits to strong piezoelectricitiy, while the large oxygen octahedron tilt helping enhancing the stability of the *P4bm* structure during changing temepraure according to the *in-situ* high-energy synchrotron X-ray diffraction measurements provides the foundation to the excellent thermal stability (20 °C-100 °C) of the piezoelectric properties. It is that a single tetragonal phase with tiny axial ratio and large oxygen octahedron tilt is an effective method to balance the piezoelectricity and thermal stability in lead-free systems.

Introduction

Lead-free piezoceramics, typically represented by $(K_{0.5}Na_{0.5})NbO_3$ (KNN)[1], $(Bi_{0.5}Na_{0.5})TiO_3$ (BNT)[2], and $BaTiO_3$ (BT)[3] -based perovskite solid solutions, have taken much attention due to nontoxic elements in nature and good piezoelectric performance, in order to compare with PZT systems or replace the lead-based counterparts. The fundamental approach in most lead-based systems for improving piezoelectricity constructs the composition-induced ferroelectric phase transition coexisting ferroelectric tetragonal and rhombohedral (T and R) phases, widely known as morphotropic phase boundary[4] (MPB). Different from the MPB in lead-based ceramics, lead-free systems exist the phase coexistence with the variation of not only composition but also temperature, which is referred to the polymorphic phase boundary[5] (PPB). Even though improved piezoelectricity has been widely reported in KNN and BT based lead-free ceramics by forming PPB between R, T, or orthorhombic (O) phase owing to vanishing energy anisotropy, undesirable thermal instability[6] of piezoelectricity could be detected simultaneously. In BNT-based lead-free ceramics, a MPB with the presence of low depolarization temperature (T_d ~ 70-100 °C) and high coercive field (E_C ~ 3-4 kV/mm) is the main factor to cause the deterioration of piezoelectric performance (d_{33} ~ 160-220 pC/N)[7]. Therefore, it is imperative demands to improve temperature stability based on good piezoelectricity in most lead-free piezoelectric materials.

In recent researches, it is an effective means that shifts the polymorphic phase transition temperature below room temperature can boot the temperature insensitivity in KNN-based ceramics. For instance, $CaTiO_3$-modified KNN–$LiSbO_3$ (d_{33} ~ 210 pC/N)) exhibits good temperature stability in the temperature range of -50 °C ~ 200 °C within single *P4mm* phase zone[8]. While, the deterioration of piezoelectricity is exhibited in pure tetragonal perovskite structure because of the lack of phase boundary causing suppressed domain wall motions because of the structural distortion[6]. In addition, the using of potassium oxide (K_2O) restricts by its drawbacks of high volatility during sintering process and strong hydroscopicity at ambient temperature[6], which leads to the difficulty in the synthesis of KNN-based systems. In order to solve the contradiction between excellent thermal stability and good piezoelectricity in lead-free systems, increased attention has been paid on $NaNbO_3$ (NN)-based perovskites. NN is well known antiferroelectric structure with *Pbcm* space group at room temperature as well as complex oxygen octahedron tilting system[9]. Tetragonal phase can be found in NN-$BaTiO_3$ (NN-BT) binary system at room temperature in the low BT content region[10]. After the addition of another ABO_3 perovskites, such as $CaZrO_3$ (CZ)[11], $BaZrO_3$ (BZ), $NaSbO_3$ (NS) and $BiFeO_3$ (BF)[12] into NN-BT, promising ferroelectric and piezoelectric properties with d_{33} ~ 200~300 pC/N as well as excellent thermal stability have been realized, which is reported to be ascribed to coexistence of *R3c* and *P4mm* phases in a wide temperature range. The NN-BT-ABO_3 systems exhibit large potential for replacing Pb-based materials if the piezoelectricity could be further improved.

The complex oxygen octahedron tilting feature in NN should be related to its low tolerance factor (t) ~0.967[13]. The addition of

[a] Beijing Advanced Innovation Center for Materials Genome Engineering, and Department of Physical Chemistry, University of Science and Technology Beijing, Beijing 100083, China
[b] School of Mathematics and Physics, University of Science and Technology Beijing, Beijing 100083, China
[c] X-ray Science Division, Argonne National Laboratory, Argonne, Illinois 60439, United States

BT in NN would lead to the disappearance of antiferroelectricity, yet part of oxygen octahedron tilting feature would be still retained. In this work, $BaSnO_3$ (BS) with relatively large tolerance factor was doped into NN-BT to modify the lattice distortion behavior. Sn is a common doping element in lead-free ceramics, which can destroy long-range ordered arrangement and form dielectric relaxation[14]. The substitution of Sn is possibly capable to induce the weaken tetragonality and introduce dielectric relaxation in NN-BT. Intriguingly, an excellent piezoelectricity (d_{33} ~ 354 pC/N) and favorable thermal stability have been achieved in 0.89NN-0.08BT-0.03BS. The large piezoelectric performance with good temperature stability derives from a *P4bm* phase with tiny tetragonality but thermal insensitive oxygen tilting behavior.

Experimental procedures

The ternary ceramics of (1-*x*-*y*)NN-*y*BT-*x*BS (x = 0-0.04 and y = 0.07-0.11) were prepared by a conventional solid-state reaction. The Na_2CO_3 (99.8%, 497-19-8, Aladdin, Shanghai), Nb_2O_5 (99.9%, 1313-96-8, Aladdin, Shanghai), $BaCO_3$ (99.95%, 12047-27-7, Aladdin, Shanghai), TiO_2 (99.8%, 13463-67-7, Aladdin, Shanghai) and SnO_2 (99.95%, 18282-10-5, Aladdin, Shanghai) were chosen as raw materials. All raw materials were dried at 300 °C for 2 hours before using. A stoichiometric amount of oxides were fully mixed with alcohol for 12 hours by planetary ball milling. The mixed powders were dried and then calcined at 900 °C for 5 hours. Then, the calcined powders were ball-milled for 24 hours again. The dried powers followed by uniaxial pressing into cylindrical pellets with polyvinyl alcohol (PVA) at a pressure of 300MPa into green pellets. The pressed pellets were sintered at 1220-1260 °C for 2 hours in a covered crucible after burning off the PVA at 550 °C for 2 hours. To reduce the volatilization of Na during sintering, the green compacts were embedded by the calcined powder with the same corresponding composition. The as-sintered disks were polished and sputtered with Au electrodes (ETD2000, Elaborate Technology Development, Beijing) for dielectric, ferroelectric and piezoelectric measurements. Ceramic disks were poled under a direct electric field of about $3E_C$ for 15min in a silicon oil bath at room temperature.

The phase structure was analyzed by synchrotron X-ray diffraction (SXRD) of 0.89NN-0.08BT-0.03BS from 25-200 °C, which was collected at the beamline 11-ID-C of APS with high-energy X-ray radiation (λ = 0.1173Å). Rietveld refinements were performed by using the program Fullprof. The dielectric permittivity was measured with a LCR meter (E4980, Agilent, Santa Clara, CA) under 0.5V at frequencies of 0.1 kHz, 1 kHz, 10 kHz, 100 kHz and 1 MHz, respectively. The polarization versus electric field loops and bipolar/unipolar strain versus electric field curves were measured at 1Hz with a triangular waveform by using ferroelectric measuring system (aixACCT, TF Analyzer 1000, Aachen, Germany). The microstructures were analyzed using scanning electron microscope (FE-SEM; LEO1530, ZEISS SUPRA 55, Berkochen, Germany). A quasi-static d_{33} meter was used to measure the piezoelectric coefficient d_{33} (China Academy of Acoustics, ZJ-3). The remanent d_{33} values were measured at room temperature after annealing at different temperature for 30 minutes. The piezoresponse force microscope (PFM) images were performed by an AFM (MFP-3D, Asylum Research, USA). The PFM sample was polished by 0.25μm polishing paste after rubbing under 2000-7000 mesh sandpapers until without obvious scratches under 3000 times optical microphotograph.

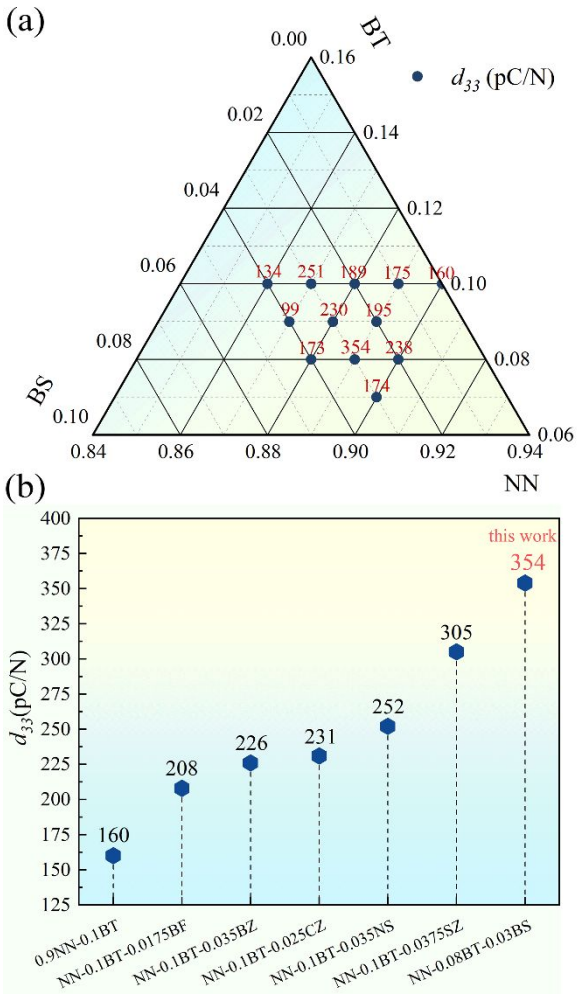

Fig. 1. (a) The room temperature d_{33} of NN-BT-BS ceramics, (b) a comparison of the d_{33} values for the present 0.89NN-0.08BT-0.03BS and other NN-based systems.

Results and discussion

After compositional optimizing of NN-BT-BS ternary system, it is intriguing that a large d_{33} value up to 354 pC/N was generated in the composition of 0.89NN-0.08BT-0.03BS, as shown in Fig. 1. The d_{33} value in this work is more than twice that of NN-BT binary ceramics (~160 pC/N) and superior to other results in the previously reported NN-based ternary ceramics[12], such as 0.865NN-0.1BT-0.035BZ (226 pC/N), 0.865NN-0.1BT-0.035NS (252 pC/N). The high piezoelectricity of this studied material is also comparable with undoped PZT ceramics (223 pC/N)[4], accelerating the process for lead-free at last[15].

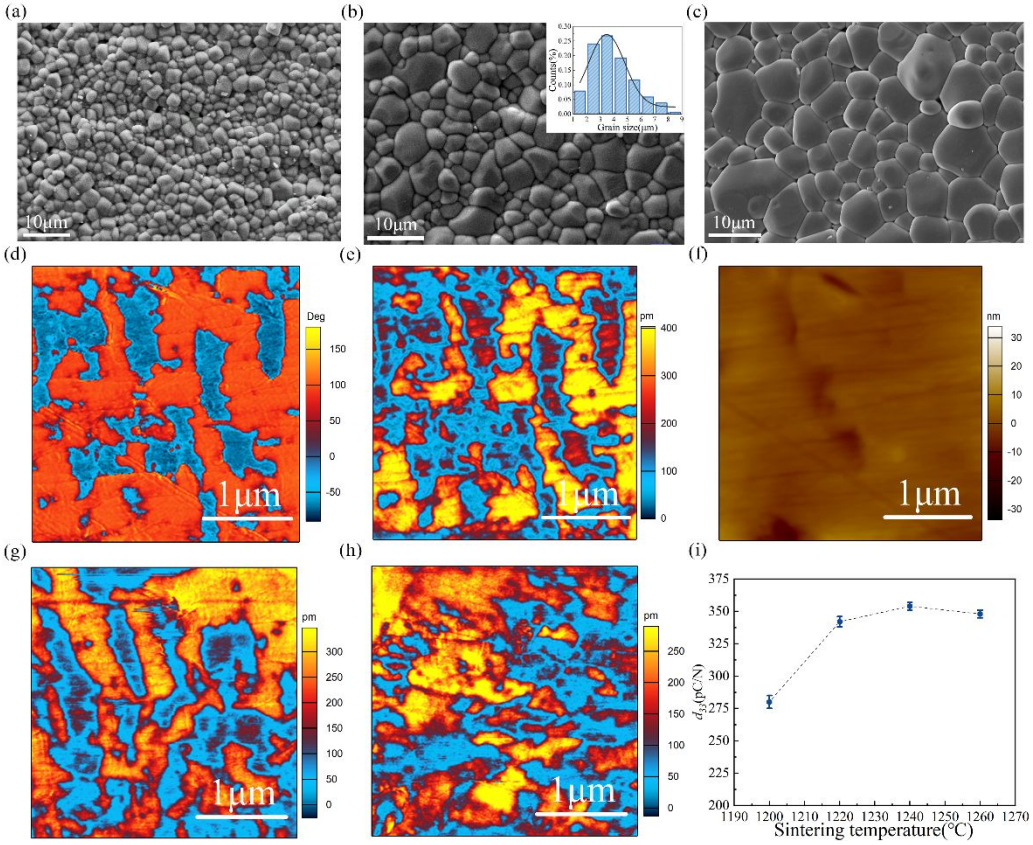

Fig. 2. (a) SEM micrograph on as-sintered surface under different sintering temperature at (a)1220 °C, (b)1240 °C, (c) 1260 °C. The inset of (b) shows the grain size distribution in SEM micrograph. (d) PFM phase image, (e) PFM amplitude image and (f) PFM surface topography of the 0.89NN-0.08BT-0.03BS ceramic sintered at 1240 °C. PFM amplitude image of the 0.89NN-0.08BT-0.03BS ceramic sintered at (g) 1220 °C and (h) 1260 °C. (i) Quasi-static d_{33} of the 0.89NN-0.08BT-0.03BS ceramic sintered at different temperatures.

Furthermore, the present lead-free ceramic of 0.89NN-0.08BT-0.03BS exhibits a good sintering property. Large d_{33} over 340 pC/N can be obtained after sintering in a wide temperature window of 1220 °C ~1260 °C, as shown in Fig. 2(i). It demands that the relatively wide range of sintering temperature is very useful for the practical application of lead-free materials. As a comparison, KNN-based ceramics require a precise sintering temperature window within 10 °C mainly due to the problem coming from the evaporation of alkali elements. Hence, unavoidable compositional fluctuation and nonuniformity owing to the exist of K element lead to a big challenge to obtain highly dense bulk samples by traditional sintering process in KNN system[6]. The stable temperature sintering property in NN-based ceramics is important development for extensive industrial applications.

The insensitive piezoelectric properties to the sintering behavior might be correlated to the microstructure, as shown in Figs. 2(a-c) for the surface morphologies of SEM pattern in 0.89NN-0.08BT-0.03BS composition sintered at different temperature. A dense microstructure with relative density more than 98% according to Archimedes method can be detected for the samples sintered at 1220-1260 °C. The apparent sphere-like grains in the 0.89NN-0.08BT-0.03BS ceramic display the equiaxed structure like most Pb-based perovskite piezoelectric ceramics, in contrast to the cubic-like grains with sharp edges in NN-BT[16] which is resemble to the typical intergranular features for KNN-based ceramics[6]. The cubic grain morphology reduces the density of the sintering ceramic and affects its smoothness. Different from the abnormally grown cubic-like grains in NN-BT[16], the addition of Sn element eliminates oversized grains, giving rise to the distribution of grain size with homogeneous grain size approximately 3.7 μm for the ceramic sintered at 1240 °C. The grain size distribution in the SEM micrograph has been shown in the inset of Fig. 2(b) that mainly presents in the range of 2-5 μm without abnormal grown. Meanwhile, the distinct difference of grain size displays the slightly growing with increasing temperature owing to thermodynamic factors. The modification of grain morphology after adding BS additives is helpful to research the processing technology of lead-free piezoelectric ceramics which is similar to traditional Pb-based perovskite system in some aspects. Apart from the grain morphology, domain structure of the 0.89NN-0.08BT-0.03BS sintered at 1240 °C was also revealed by PFM in Figs. 2(d) and 2(e). Lamellar domains, which is widely found in tetragonal phase, with width <100 nm can be clearly seen from both PFM amplitude and phase images. The nanosized domains are thought to be benefit to the piezoelectricity owing to the easy domain wall motion under external stimulation[17]. Significantly, the surface topography is provided in Fig. 2(f) which is obviously different from the fronts. It is shown that the surface state of PFM samples hardly affects the domain structures. The PFM amplitude images for the 0.89NN-0.08BT-0.03BS samples sintered at different temperatures also exhibit the similar domain morphology, as shown in Figs. 2(g) and 2(h). The homologous

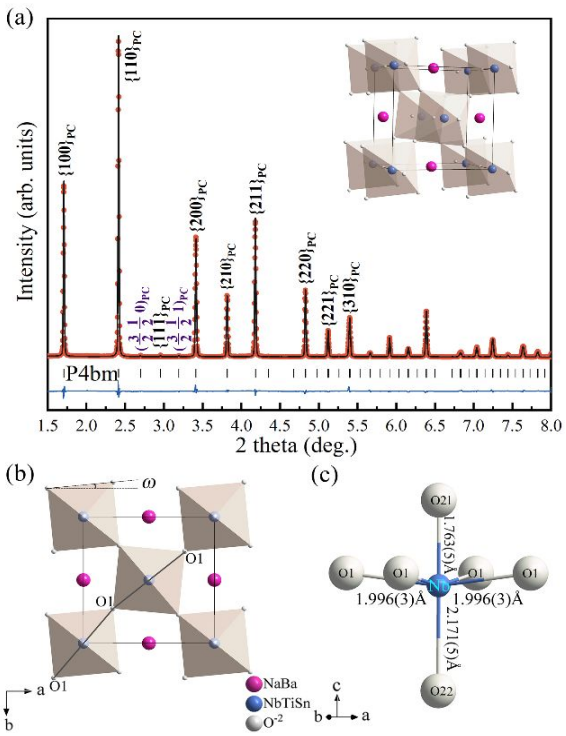

Fig. 3. (a) Structural refinement of high energy synchrotron powder diffraction of 0.89NN-0.08BT-0.03BS at room temperature. The red circles correspond to the raw diffraction data, black line indicates the calculated diffraction pattern, and the black vertical ticks mark the Bragg positions of *P4bm* reflections. The pseudo-cubic peaks are used in order to compare with perovskite structure. The purples sign the superstructure peaks of *P4bm* phase. The inset shows the *P4bm* structure. (b) Projection of the 0.89NN-0.08BT-0.03BS structure on *ab* plane. (c) The diagram of Nb-O octahedron.

microstructures of ceramics under wide sintering temperature thoroughly explain the insensitive behavior of d_{33}.

Full profile of SXRD pattern was taken to analyze the phase structure of 0.89NN-0.08BT-0.03BS ceramic, and a single perovskite structure can be identified according to the Rietveld refinement[18] shown in Fig. 3(a). The Rietveld refinement reveals that the structure model of *P4bm* yields the best agreement, which indicates that the present composition of 0.89NN-0.08BT-0.03BS is a single tetragonal phase. This *P4bm* structure features an oxygen octahedron rotation in *ab* plane along the axis of *c*, briefly named $a^0a^0c^+$ according to the Glazer notation[19], which is partly analogous to parent NN structure. It needs to note that it is the first time to identify *P4bm* symmetry[20] in the NN-BT based polycrystalline ceramics, which were previously assumed as *P4mm*[10, 12]. The *P4bm* model (R_{wp}=6.87%) can yield a better agreement than that of the *P4mm* model (R_{wp} = 7.48%)[3]. Moreover, correlative characteristic superlattice peaks such as $(\frac{3}{2}\ \frac{1}{2}\ 0)$ and $(\frac{3}{2}\ \frac{1}{2}\ 1)$ can be clearly seen in Fig. 3(a), which should be related to the oxygen octahedron rotation feature for the *P4bm* structure instead of *P4mm*. The refined structural parameters are summarized in Table 1. The unit cell parameters $a = b = 5.571(23)$ Å are about $\sqrt{2}$ times of the perovskite cell, and the *c* axis is 3.933(86) Å which is smaller than that of tetragonal BT ($c = 4.05$ Å, *P4mm*)[21]. The tetragonality of the present composition can be calculated as $a/(c*\sqrt{2}) \sim 1.001(57)$. As a comparison, the reduced tetragonality has already reported in the BT-based lead-free

Table 1. The detailed structure parameters of tetragonal 0.89NN-0.08BT-0.03BS refined by the Rietveld method.

0.89NN-0.08BT-0.03BS					
Space group *P4bm*		$a = 5.571(23)$Å $c = 3.933(86)$Å		$R_p = 6.15\%$ $R_{wp} = 6.87\%$	
Atom	**X**	**Y**	**Z**	**Occ**	**Biso**
Na^{+1}	0	0.5	0.49(75)	0.89	1.2(69)
Ba^{+2}	0	0.5	0.49(75)	0.11	1.2(69)
Nb^{+5}	0	0	0	0.89	0.77(1)
Ti^{+4}	0	0	0	0.08	0.77(1)
Sn^{+4}	0	0	0	0.03	0.77(1)
O^{-2}	0.273(95)	0.226(06)	0.065(83)	2	1
O^{-2}	0	0	0.44(82)	2	1

system, such $0.5Ba(Ti_{0.8}Zr_{0.2})O_3$-$0.5(Ba_{0.7}Ca_{0.3})TiO_3$ with a small $c/a \sim 1.005$ accompanied the large piezoelectric coefficient (620 pC/N)[3]. Smaller axial ratio means the smaller lattice distortion similar to cubic-like lattices[22]. It benefits for domains switching during poling process and polarization reorientation along electric field, generally implying higher domain wall mobility, which corresponds to enhanced piezoelectric response[23]. A very small lattice distortion can be observed in the 0.89NN-0.08BT-0.03BS, which provides the basic for the improved piezoelectricity owing to the enhanced domain switching.

Different from the symmetry of *P4mm* in earlier reports, oxygen octahedral tilting and rotation occur in the perovskite of *P4bm* phase. The tolerance factor of the studied sample is calculated approximately 0.976. It is usually believed that oxygen octahedral rotation is likely to exist due to small $t < 1$ in perovskite when the radii of A-site ions are relatively diminutive, such as BNT-based compositions (*t* is below 0.985). The rotation of oxygen octahedrons can effectively optimize the coordination environment of A-site to stabilize the perovskite structure. Small ions of Na are not large enough to fill in the steric linkage of NbO_6 framework, which promotes the octahedral rotation for the favor energy. In other respect, *P4bm* structure prefers to exhibit the weak ferroelectric distortion with *c/a* tending to 1 accompanied by small spontaneous polarization[24], in comparison to a large tetragonality and polarization in *P4mm* phase[25]. In conclusion, the 0.89NN-0.08BT-0.03BS compound is likely to emerge *P4bm* structure rather than *P4mm* phase.

The origin of ferroelectricity is induced by the relative displacements between cations and anions, leading to a net dipole moment of polarization[26]. In the present 0.89NN-0.08BT-0.03BS, bond length as well as the degree of distortion can be extracted from the *P4bm* distorted NbO_6 octahedron (Figs. 3(b) and (c)), which contain three different Nb-O distances of the longest Nb-O22 (~2.171(5) Å), the four middle Nb-O1 (~1.996(3) Å), and the shortest Nb-O21 (~1.763(5) Å). The distortion angle ω calculated by the inclination of O1-O1-O1 is ~5.4(6)°. The Nb-O bond length between the longest and the shortest one is up to 0.408Å, resulting in the Nb off-center displacement about 0.260 Å in the oxygen octahedron. Therefore, spontaneous polarization (P_S) can be basically estimated by assuming standard atomic ionization states ($P_S \sim 33.549\ \mu C/cm^2$). Compared with common *P4bm* phase with the antiparallel off-center displacement between the A- and B-site atoms in BNT-based ceramic[23], the 0.89NN-0.08BT-0.03BS displays a parallel polar displacement

orientation in both A and B sites with large P_S, which is favor to the high piezoelectric performance.

The temperature and frequency dependent dielectric permittivity (ε_r) and dielectric loss (tanδ) values of 0.89NN-0.08BT-0.03BS ceramic are displayed in Fig. 4(a). A relatively smooth curve and only one anomalous dielectric peak occur around $T_m \sim 120$ °C similar to studied other NN-BT systems (80 °C ~150 °C), representing the ferroelectric-to-paraelectric phase transition without other structural changes. It is worth noting that the diffuse phase transition phenomenon and frequency dispersion of dielectric peaks display a typical dielectric relaxation[27]. The equivalently crystallographic sites with different radius and valence ions, such as A-site occupied by Na^+ and Ba^{2+}, B-site located by Nb^{5+}, Ti^{4+} and Sn^{4+}, induce the constituent disorder causing relaxor ferroelectrics. The variation of local Curie temperatures is responsible for the diffuse phase transition behavior of the typical relaxor ferroelectric characteristic[13]. The appearance of dielectric relaxation would be favor to the piezoelectricity as well as temperature stability, which can be proved by the temperature dependent piezoelectric properties in Fig. 4(d). The small-signal d_{33} remains less than 5% from room temperature to the temperature very close to its T_m. It is worth of noting that the relative variation of d_{33} in the measured temperature range is much smaller than other lead-free phase-boundary systems which exhibit the fluctuation about 20% within the temperature 100 °C[28-32]. Such as KNN-based ceramics, the PPB affects the variation of phase composition with changing temperature, which causes temperature-sensitive piezoelectric properties particularly in the compositions of close to PPB. The temperature stability of piezoelectric properties affected by PPB have been improved by some methods, such as shifting the $T_{O\text{-}T}$ below room temperature by chemical modifications or producing highly textured ceramic samples[17], however, most researches take more attention on the enhanced temperature stability in regard to unipolar strain behavior, namely the large-signal d_{33}^*, not the small-signal d_{33}. The almost constant piezoelectric property in the overall ferroelectric interval found in this work shows large potential application prospects in precision device.

The temperature dependence of polarization hysteresis (*P-E*) and unipolar strain (*S-E*) are obtained in Figs. 4(b) and 4(c), respectively. Well-saturated *P-E* loops and unipolar *S-E* curves indicate a typical macroscopical ferroelectric state at room temperature. The maximal polarization (P_{max}) is about 25 μC/cm^2 at 3 kV/mm, which is smaller than the theoretical value obtained by Rietveld refinements. This might be contributed to the restriction such as defects, incomplete domain switching and heterogeneous grain size[23]. The remanent polarization (P_r) is about 16 μC/cm^2, while a small E_C is 1 kV/mm at ambient temperature. Polarization and E_C present a similar tendency to deterioration gradually with increasing temperature in Fig. 4(e), implying the reduced spontaneous polarization and approaching to the ferroelectric-to-paraelectric phase transition. Large-signal piezoelectric coefficient of d_{33}^* calculated by the slope of unipolar *S-E* loops is approximately 327 pm/V at room temperature. The unipolar strain exhibits a slight decrease with increasing temperature in Fig. 4(f) showing the change of d_{33}^* in ceramic. It is noted that the relative high unipolar strain is still observed up to T_m, which should be due to the high piezoelectricity at low temperature range and high electrostriction close to T_m[33]. Moreover, a very small hysteresis

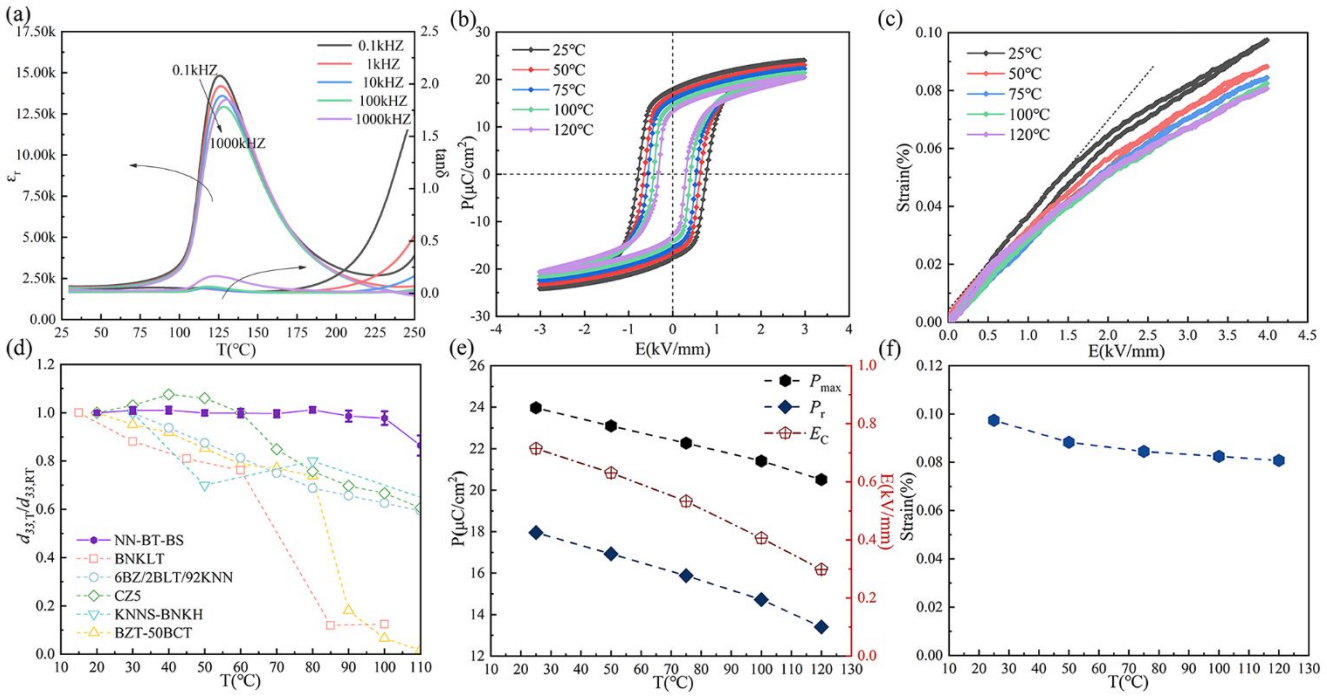

Fig. 4. (a) Dielectric permittivity and loss tangent as a function of temperature and frequency. (b) Temperature-dependent polarization loops of the 0.89NN-0.08BT-0.03BS composition measured at 3 kV/mm. (c) Unipolar strain of the 0.89NN-0.08BT-0.03BS ceramic under 4 kV/mm at different temperatures. (d) The temperature dependence of d_{33} values relative to the RT ones for the present composition and some typical lead-free materials[28-32]. (e) The maximum polarization (P_{max}), the remanent polarization (P_r) and coercive field (E_C) at various temperatures. (f) Evolution of unipolar strain with temperature.

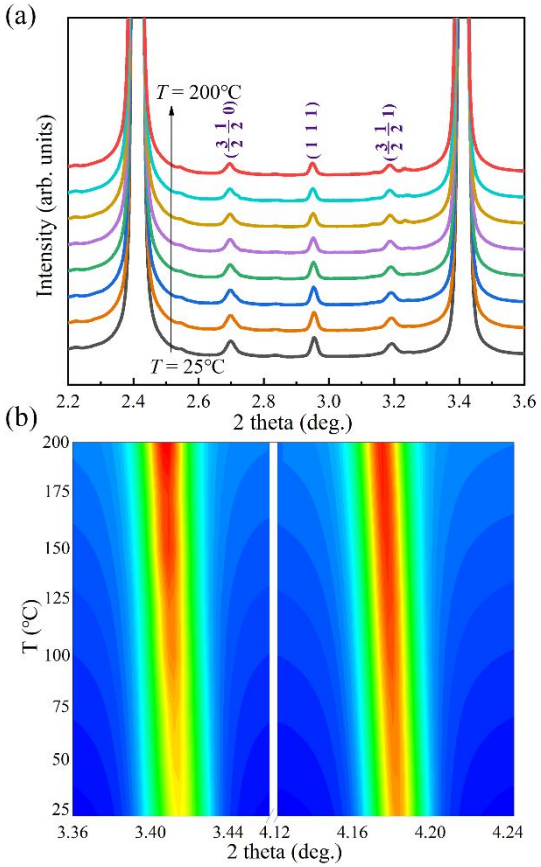

Fig. 5. The temperature-dependent synchrotron X-ray diffraction patterns for 0.89NN-0.08BT-0.03BS at increasing temperature (25 °C -200 °C) shown the enlarged profile of (a) 2.2 to 3.6 and (b) 3.36 to 4.24.

is observed (<10%) in the studied temperature range, which is unavailable in field-induced phase transition ceramics, such as BNT and BNT-BKT-KNN with large strain but high hysteresis (>50%)[34]. This should be conferred by the hysteresis-free feature of both piezoelectric and electrostrictive effect[10]. The temperature insensitive low hysteresis large strain makes the studied material to be advantage for using in high-precision actuators.

To further reveal the excellent temperature stability essentially, high-energy SXRD patterns of 0.89NN-0.08BT-0.03BS ceramic measured with varied temperature from 25 °C to 200 °C. *P4bm* phase remains up to 200 °C on heating, which could be clearly reflected on the existence of $(\frac{3}{2}\ \frac{1}{2}\ 0)$ and $(\frac{3}{2}\ \frac{1}{2}\ 1)$ superlattice profiles in the studied temperature range in Fig. 5(a). It is interesting noted that the *P4bm* phase is still stable beyond T_m ~120 °C. This is a common phenomenon in relaxor ferroelectrics that the dynamic and size of domains change drastically around T_m but the local symmetry does not change, which would also lead to the change from polar state to nonpolar state from the macroscopic structure point of view[27]. Even though little change on the phase structure can be detected on heating, the parameters of the perovskite unit cell change obviously, as revealed on the change of $(200)_{PC}$ and $(211)_{PC}$ diffraction lines in Fig. 5(b). The evolution of lattice parameters gained from Rietveld refinement results are shown in Fig. 6.

The increase of $a/\sqrt{2}$ axis and c axis displays a normal linear positive expansion (Fig. 6(a)) as changing temperature, yet the calculated axial radio $a/(c*\sqrt{2})$ in perovskite unit cell decreases from 1.001(57) at room temperature to ~1 above 120 °C, indicating the decreased tetragonality during heating. It is worth nothing that the octahedral distortion degree keeps nearly

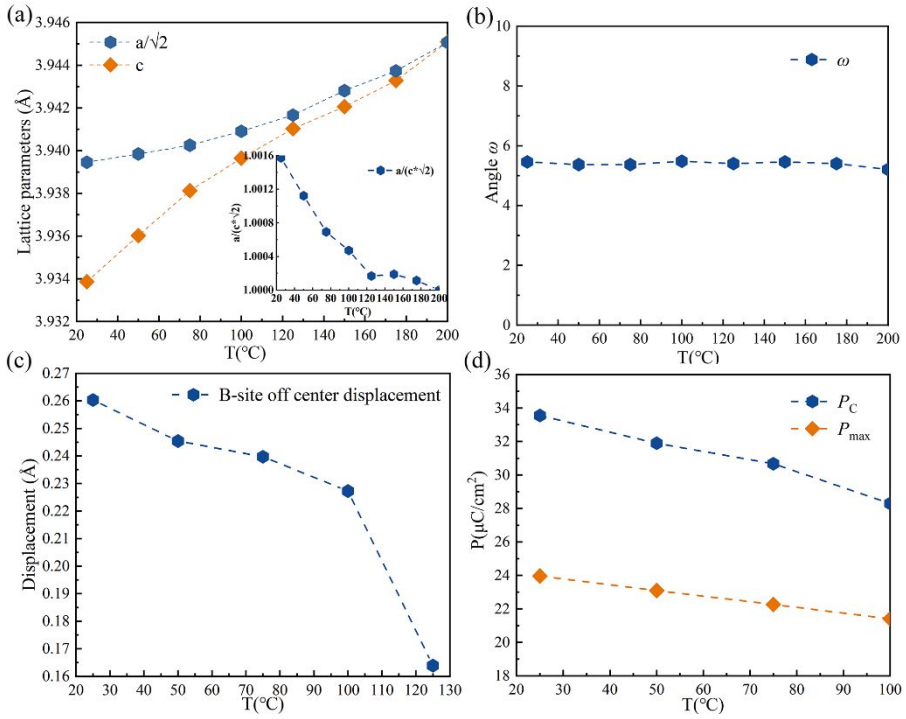

Fig. 6. Temperature dependence of (a) lattice parameters, (b) angle ω of distortion, (c) B-site off center displacement and (d) polarization of calculated and measured values in the composition of 0.89NN-0.08BT-0.03BS. The inset of (a) shows the changing of axial ratio with temperature.

unchanged, leading to a tiny fluctuation of angle ω in *ab* plane near 5.4° in Figure 6(b). The existence of oxygen octahedral tilting in perovskites is thought to be bad for piezoelectric properties[35]. However, the large oxygen octahedral distortion angle makes the phase quite stable with changing temperature, leading to the existence of *P4bm* phase in a wide temperature range even above depolarization temperaure[35] and providing the basic for thermal stable piezoelectric response. The long range ordered ferroelectric domains are broken into polar nanoregions on heating, leading to the disappearance of macroscopic polarization. Significantly decreased B-site off-centering displacement can also be found close to T_m, resulting in the theoretical spontaneous polarization value. In the temperature range below T_m, calculated polarization exhibits a slight shrinking result from 33.549 μC/cm^2 to 28.293 μC/cm^2 in the ferroelectric phase region, contributing to the temperature-insensitive ferroelectricity. The *P4bm* phase with tiny distortion in NN-based ceramics demonstrates the large piezoelectric performance and excellent temperature stability.

Conclusions

In summary, the relationship between phase structure and electrical properties for the 0.89NN-0.08BT-0.03BS ceramic is investigated in detail in this work. *In situ* high-energy SXRD patterns indicate that the present ceramic exhibits a tetragonal phase with *P4bm* symmetry in a wide temperature range from 25 °C to 200 °C, even though the transition into nonpolar relaxor ferroelectric phase leading to a decreased spontaneous polarization occurs at around T_m~120 °C. The small axial ratio feature of *P4bm* structure below T_m leads to a large piezoelectric response with d_{33} up to 354 pC/N and a nonhysteretic unipolar strain simultaneously in 0.89NN-0.08BT-0.03BS ceramic, while the large oxygen octahedral tilting provides the basic for the temperature insensitive phase structure as well as piezoelectric properties in the range of 20 °C - 100 °C. The results found in this work can put forward a meaningful thought that the single tetragonal phase with tiny axial ratio and large oxygen octahedral distortion can simultaneously improve the piezoelectricity and temperature stability in lead-free ceramics.

Acknowledgements

This work was supported by the National Natural Science Foundation of China (grant nos. 21825102, 22075014, and 22001014), the Fundamental Research Funds for the Central Universities, China (FRF-TP-18-001C2); National Postdoctoral Program for Innovative Talents (BX20200044, and BX20200043); and the State Key Lab of Advanced Metals and Materials (2020-ZD01). This research used resources of the Advanced Photon Source, a US Department of Energy (DOE) Office of Science User Facility operated for the DOE Office of Science by Argonne National Laboratory under Contract No. DE-AC02-06CH11357.

Notes and references

1 Y. Saito, H. Takao and T. Tani, *Nature*, 2004, **432**, 84.
2 T. Takenaka, K. Aruyama and K. Sakata, *Jpn. J. Appl. Phys.,* 1991, **30**, 2236.
3 W. Liu and X. Ren, *Phys. Rev. Lett.*, 2009, **103**, 257602.
4 B. Jaffe, *Piezoelectric ceramics*, Elsevier, 2012.
5 Y. Dai, X. Zhang and G. Zhou, *Appl. Phys. Lett.*, 2007, **90**.
6 J.-F. Li, K. Wang, F.-Y. Zhu, L.-Q. Cheng, F.-Z. Yao and D. J. Green, *J. Am. Ceram. Soc.*, 2013, **96**, 3677-3696.
7 J. Wu, in *Advances in Lead-Free Piezoelectric Materials*, Springer, 2018, pp. 191-245.
8 S. Zhang, R. Xia and T. R. Shrout, *Appl. Phys. Lett.*, 2007, **91**.
9 L. Jiang, D. C. Mitchell, W. Dmowski, and T. Egami, *Phys. Rev. B*., 2013, **88**, 014105.
10 X. Lu, L. Hou, L. Jin, L. Wang, Y. Tian, K. Yu, Q. Hu, L. Zhang and X. Wei, *Ceram. Int.*, 2018, **44**, 5492-5499.
11 R. Zuo, H. Qi and J. Fu, *Appl. Phys. Lett.*, 2016, **109**.
12 H. Qi, R. Zuo, J.-f. Li and L. Li, *J. Eur. Ceram. Soc.*, 2018, **38**, 5341-5347.
13 I. Grinberg and A. M. Rappe, *Phase Transitions*, 2007, **80**, 351.
14 T. Shi, L. Xie, L. Gu and J. Zhu, *Sci. Rep.*, 2015, **5**, 8606.
15 E. Cross, *Nature*, 2004, **432**, 24-25.
16 J. T. Zeng, K. W. Kwok and H. L. W. Chan, *J. Am. Ceram. Soc.*, 2006, **89**, 2828-2832.
17 F.-Z. Yao, K. Wang, W. Jo, K. G. Webber, T. P. Comyn, J.-X. Ding, B. Xu, L.-Q. Cheng, M.-P. Zheng, Y.-D. Hou and J.-F. Li, *Adv. Funct. Mater.*, 2016, **26**, 1217-1224.
18 H. Liu, J. Chen, L. Fan, Y. Ren, L. Hu, F. Guo, J. Deng and X. Xing, *Chem. Mater.*, 2017, **29**, 5767-5771.
19 A. M. Glazer, *Acta Crystallogr. Sect. B: Struct. Crystallogr. Cryst. Chem.*, 1972, **28**, 3384-3392.
20 L. Gacem, D. Ouadjaout, J.-P. Chaminade, M. Maglione, R. Von der Mühll and S. Pechev, *Mater. Res. Bull.*, 2009, **44**, 2240-2245.
21 M. Acosta, N. Novak, V. Rojas, S. Patel, R. Vaish, J. Koruza, G. A. Rossetti and J. Rödel, *Appl. Phys. Rev.*, 2017, **4**.
22 Y. S. Sung, J. M. Kim, J. H. Cho, T. K. Song, M. H. Kim, and T. G. Park, *Appl. Phys. Lett.*, 2010, **96**, 202901.
23 H. Liu, J. Chen, H. Huang, L. Fan, Y. Ren, Z. Pan, J. Deng, L. Q. Chen and X. Xing, *Phys. Rev. Lett.*, 2018, **120**, 055501.
24 Y. Kitanaka, M. Ogino, K. Hirano, Y. Noguchi, M. Miyayama, Y. Kagawa, C. Moriyoshi, Y. Kuroiwa, S. Torii and T. Kamiyama, *Jpn. J. Appl. Phys.*, 2013, **52**.
25 Y. Kitanaka, M. Ogino, Y. Noguchi, M. Miyayama, A. Hoshikawa and T. Ishigaki, *Jpn. J. Appl. Phys.*, 2018, **57**.
26 R. E. Cohen, *Nature*, 1992, **358**.
27 A. A. Bokov and Z. G. Ye, *J. Mater. Sci.*, 2006, **41**, 31-52.
28 S. Lu, Z. Xu, S. Su and R. Zuo, *Appl. Phys. Lett.*, 2014, **105**.
29 K. Wang, F.-Z. Yao, W. Jo, D. Gobeljic, V. V. Shvartsman, D. C. Lupascu, J.-F. Li and J. Rödel, *Adv. Funct. Mater.*, 2013, **23**, 4079-4086.
30 R. Wang, K. Wang, F. Yao, J.-F. Li, F. H. Schader, K. G. Webber, W. Jo, J. Rödel and S. Zhang, *J. Am. Ceram. Soc.*, 2015, **98**, 2177-2182.
31 B. Zhang, J. Wu, B. Wu, D. Xiao and J. Zhu, *J. Alloys Compd.*, 2012, **525**, 53-57.
32 T. Zheng, H. Wu, Y. Yuan, X. Lv, Q. Li, T. Men, C. Zhao, D. Xiao, J. Wu, K. Wang, J.-F. Li, Y. Gu, J. Zhu and S. J. Pennycook, *Energy Environ. Sci.*, 2017, **10**, 528-537.
33 F. Li, L. Jin, Z. Xu and S. Zhang, *Appl. Phys. Rev.*, 2014, **1**, 011103.
34 S. O. Leontsev and R. E. Eitel, *Sci. Technol. Adv. Mater.*, 2010, **11**, 044302.
35 K. Yan, S. Ren, M. Fang and X. Ren, *Acta Mater.*, 2017, **134**, 195-202.

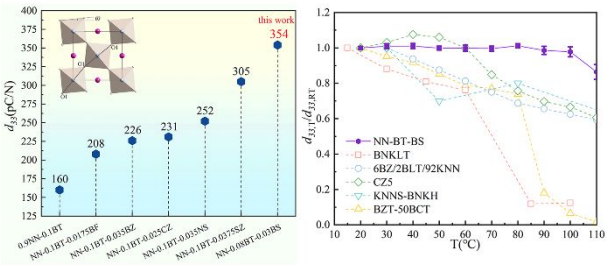

A single tetragonal phase with tiny axial ratio and large oxygen octahedron tilt obtains boosted piezoelectricity with excellent thermal stability.